Exciton and trion spectral line shape in the presence of an electron gas in GaAs/AlAs quantum wells

A. Manassen, E. Cohen, Arza Ron, and E. Linder
Solid State Institute, Technion–Israel Institute of Technology, Haifa 32000, Israel

L. N. Pfeiffer
Bell Laboratories, Murray Hill, New Jersey 07974

(Received 31 May 1996)

We studied the photoluminescence of $(e1{:}\mathrm{hh}1)1S$ excitons (X) and negatively charged excitons (trions, X^-) in quantum wells (QW's) having a low-density ($n_e<5\times10^{10}$ cm^{-2}) two-dimensional electron gas (2DEG) at $T\leqslant12$ K. Mixed type-I–type-II GaAs/AlAs quantum wells are studied in which the 2DEG is photogenerated in the type-I QW's and n_e is determined by the excitation intensity. At a given temperature and for every excitation intensity the photoluminescence spectrum is decomposed into a Lorentzian-shaped X^- line and a convoluted Lorentzian-Gaussian X line. Their intensity ratio is analyzed by assuming a thermal equilibrium distribution of X and X^- that is determined by the chemical potential of the 2DEG. The X^- linewidth dependence on n_e is analyzed as originating from an increased X^- dephasing rate that is caused by trion-electron (X^--e) scattering. We present a model of the elastic (X^--e) scattering and calculate its rate as a function of n_e assuming the 2DEG screening wave vector (q_s) to be an adjustable parameter. Although of the same order of magnitude, the fitted q_s values differ from those calculated for the ideal gas model using the Thomas-Fermi approximation. Since, to our knowledge, there is no model for calculating q_s in the low 2DEG density range studied here and $T>0$, our spectroscopically extracted $q_s(n_e)$ values might serve as guidelines for the required theory. [S0163-1829(96)03140-2]

I. INTRODUCTION

Interband transitions in quantum wells (QW's) containing a two-dimensional electron gas (2DEG) are extensively investigated.[1,2] The spectral range of the $e1$-hh1 and $e1$-lh1 interband transitions provides detailed information on both the 2DEG properties and those of the photoexcited electron-hole pair. For a dilute 2DEG ($n_e<5\times10^{10}$ cm^{-2}) and at low temperatures, the $(e1{:}\mathrm{hh}1)1S$ exciton (X) is a bound state.[3,4] Recently, bound electron-exciton particles (negative trions, X^-) were observed in CdTe (Ref. 5) and in GaAs QW's (Refs. 6–8) containing a low-density 2DEG. The reported studies include the X^- energy levels, the transition polarizations and their magnetic-field dependence, the X^- spatial localization, and the relative X and X^- densities. The data were extracted from low-temperature photoluminescence (PL) and its excitation (PLE) spectra. Two methods were used in order to vary the 2DEG density: application of a bias voltage to modulation n-doped quantum structures or depleting the 2DEG in such structures by varying the photoexcitation intensity (at an energy above the barrier). In such experiments n_e is much higher than the X^- and X densities. Therefore, it is reasonable to assume that the spectroscopic and thermodynamic properties of the three-component phase depend mainly on n_e and T.

The purpose of the present study is to examine the X and X^- homogeneous linewidth when the 2DEG density is varied in the range $10^9\leqslant n_e<5\times10^{10}$ cm^{-2} at temperatures $T\leqslant12$ K. We find that while the homogeneous linewidth of X hardly changes, that of X^- increases with n_e. This increase is interpreted as originating from an enhanced dephasing rate that is due to the interaction of electrons with X^-. Since both X^- and e are charged particles, they interact via the screened Coulomb interaction and thus our spectroscopic study utilizes the X^- linewidth as a means to learn about the screening wave-vector dependence on density, $q_s(n_e)$, in the low-n_e limit. In order to obtain a 2DEG having such low densities that can be varied continuously in the same sample, we use mixed type-I–type-II GaAs/AlAs quantum wells (MTQW's). In these undoped MTQW's, a long-lived separately confined 2DEG and a two-dimensional hole gas (2DHG) are generated in the type-I and type-II QW's, respectively, and their density is controlled by the photoexcitation intensity.[9,10] We measure the X and X^- PL spectral line-shape dependence on n_e for several temperatures and obtain their intensities and linewidths. Details are given in Sec. II. In Sec. III we analyze the relative X and X^- PL intensities assuming a thermal equilibrium determined by the 2DEG chemical potential, $\mu(n_e,T)$, and we use this assumption in order to obtain n_e as a function of the photoexcitation intensity. We then present a model for calculating the (X^--e) elastic-scattering rate. This model uses $q_s(n_e)$ as a fitting parameter. We thus calculate the rate by fitting it to the observed increase in linewidth. The extracted values of $q_s(n_e)$ are found to be higher than those calculated for an ideal 2DEG model. We conclude with a short summary.

II. EXPERIMENT

The mixed type-I–type-II GaAs/AlAs quantum-well structures were grown by molecular-beam epitaxy on undoped, [001]-oriented GaAs substrates. Their electronic structure is schematically shown in Fig. 1 by plotting the variation of the conduction bands (Γ_c and X_c) and the va-

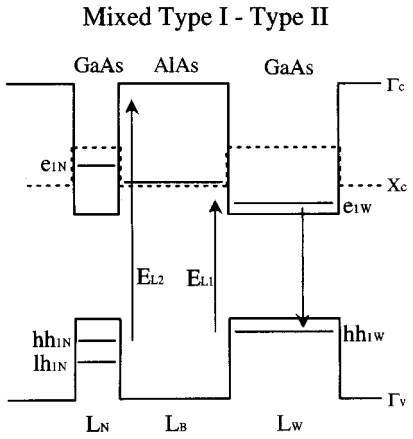

FIG. 1. Schematic description of the mixed type-I–type-II quantum well structure. L_N, L_W, and L_B are the widths of the narrow well, wide well, and barrier, respectively. The solid lines represent the spatial variation of the conduction- and valence-band edges at the Γ point of the Brillouin zone and the dotted line represents that of the X_c band.

lence band (Γ_v) along $z\|[001]$ (the growth direction). The MTQW studied here consists of 30 periods of alternating wide GaAs wells ($L_W=198$ Å) and narrow wells ($L_N=26$ Å) that are separated by AlAs barriers ($L_B=102$ Å). Galbraith *et al.*[9] and Feldman *et al.*[10] showed that under photoexcitation with $E_L>E_{e1N}-E_{\mathrm{hh1}N}$, the electrons relax rapidly from the narrow wells, through the X_c band of the AlAs barriers, and accumulate in the $e1W$ band of the wide wells. The holes tunnel slowly ($\tau_t\sim5$ msec for $L_B=102$ Å at $T=2$ K) and thus a spatial separation between the 2DEG in the wide wells and the 2DHG in the narrow wells is achieved.

We utilize[11] these properties in order to form a 2DEG with a controlled density in the wide wells by photoexciting with an Ar^+ laser, $E_{L_2}=2.41$ eV, and intensities at the sample surface of $0\leqslant I_{L_2}\leqslant 10$ mW/cm^2. In the PL experiments reported here we simultaneously photoexcited the MTQW at E_{L_2} and just above the $(e1{:}\mathrm{hh1})_W1S$ exciton band with a Ti:sapphire laser at an energy of $E_{L_1}=1.538$ eV and with a fixed intensity of $I_{L_1}=3$ W/cm^2 (cf. Fig. 1). The samples were placed in an immersion-type dewar and the temperature was varied in the range $2<T\leqslant 12$ K. The spectra were measured with a double spectrometer having a spectral resolution of 0.05 meV.

The PL and PLE spectra shown in Fig. 2 serve to identify the lines under study. The X^- line is clearly observed in the PL spectrum at $E_b=1.3$ meV below the X line. These two PL lines were studied for various temperatures and I_{L_2} values and typical spectra are shown in Fig. 3. In order to obtain the X and X^- intensities and linewidths, we fit each spectrum to a double Voigt line-shape function. This function is a convolution of a Lorentzian and a Gaussian. The results of the individual line fittings are also shown in Fig. 3 by dashed lines for the separate X and X^- lines and by a dotted line for their sum. We found that the X^- line is a pure Lorentzian for all T and I_{L_2}, while the X line has a Voigt line shape with a Gaussian (inhomogeneous) and Lorentzian (homogeneous) widths that depend on both T and I_{L_2}. The fitting yields the intensity ratio I_X/I_X- for each spectrum. This ratio as a function of I_{L_2} is presented in Fig. 4 for $T=5$, 8, and 12 K. Figure 5 presents the linewidth increment with I_{L_2} as obtained by the line-shape analysis: $\Delta\Gamma(n_e)=\Gamma(n_e)-\Gamma(0)$, where $\Gamma(n_e)$ is the linewidth obtained for a given I_{L_2} and $\Gamma(0)$ is the linewidth observed with I_{L_1} only. Note that for X,

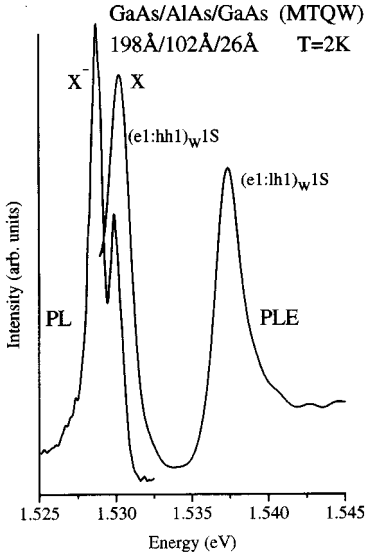

FIG. 2. PL spectrum obtained under photoexcitation into the wide wells only (at $E_{L_1}=1.538$ eV) and its excitation spectrum (PLE) monitored at the X^- line.

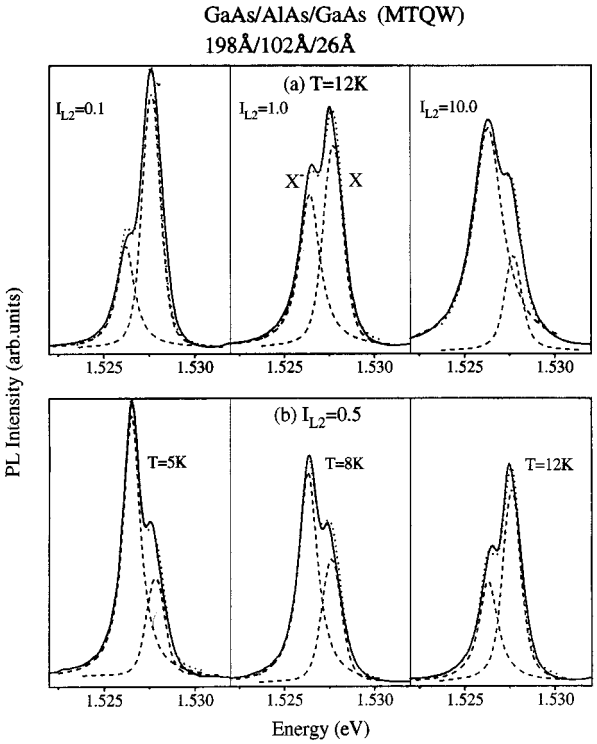

FIG. 3. (a) PL spectra observed at $T=12$ K and increasing I_{L_2}. (b) PL spectra obtained for a fixed I_{L_2} and increasing temperature. The decomposition of each spectrum into X and X^- lines (dashed lines) is described in the text. The dotted line is their sum. (I_{L_2} is given in units of mW/cm^2.)

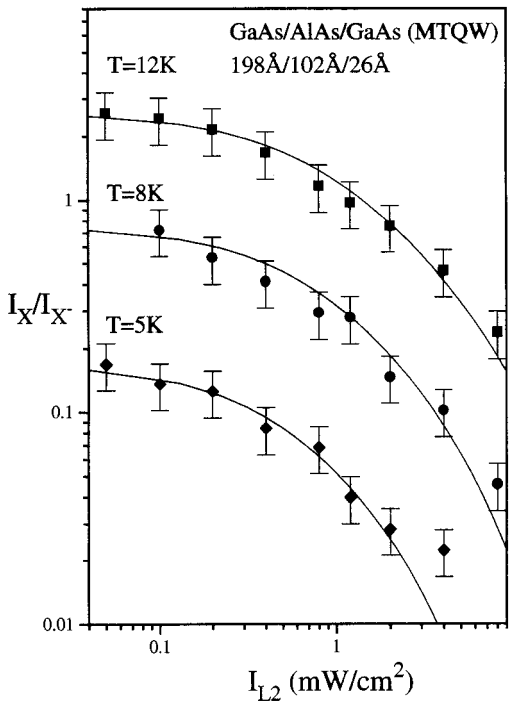

FIG. 4. Intensity ratio of the X to X^- lines as a function of I_{L_2} (namely, for various n_e) and for different temperatures. The solid lines are obtained by fitting the two-level model assuming an ideal 2DEG.

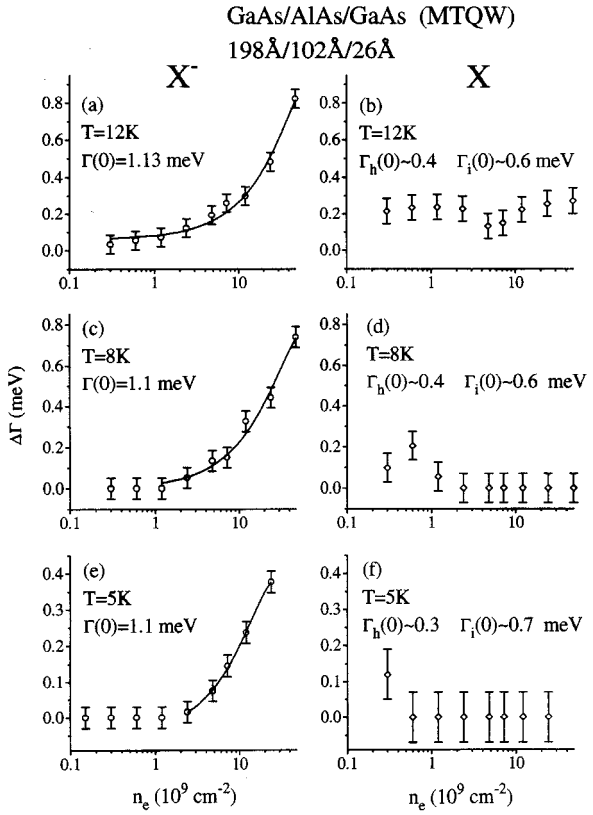

FIG. 5. X and X^- linewidth increment with n_e for different temperatures. $\Gamma(0)$ is the linewidth obtained under resonant excitation only. X^- is always a Lorentzian (homogeneous). For X, $\Gamma_h(0)$ is the initial homogeneous linewidth and $\Gamma_i(0)$ is the inhomogeneous part (of the Voigt line shape). The solid lines are model fittings as described in Sec. III.

only the homogeneous linewidth is presented [Figs. 5(b), 5(d), and 5(f)]. Also, for X^- it is found that at $T=5$ K, $\Delta\Gamma(n_e)>0$ only for $n_e>2\times10^9$ cm^{-2} [Fig. 5(e)] and at $T=8$ K this occurs already for $n_e>10^9$ cm^{-2} [Fig. 5(c)].

III. MODEL AND ANALYSIS

In this section we will analyze the experimental results shown in Figs. 4 and 5 in order to explain the variation of n_e and $\Delta\Gamma$ with increased photoexcitation intensity I_{L_2}. In order to obtain $n_e(I_{L_2})$ we follow the analysis given in Ref. 8 and assume that in the temperature and photoexcitation ranges of our experiments the system consisting of the neutral and charged excitons behaves as a two-level system in equilibrium. Moreover, we assume that the equilibrium conditions are determined by the 2DEG, namely, the chemical potential is that of the electrons given by the expression for an ideal fermion gas

$$\mu = k_B T \ln[e^{E_F/k_B T} - 1], \tag{1}$$

with $E_F = \pi\hbar^2 n_e/m$. Then, the intensity ratio is given by

$$4\frac{I_X}{I_{X^-}} = \frac{n_X}{n_{X^-}} = 4e^{(E_b-\mu)/k_B T}, \tag{2}$$

where n_X and n_{X^-} are the X and X^- densities, respectively, and the factor 4 is their degeneracy ratio. The solid curves shown in Fig. 4 are obtained by fitting Eqs. (1) and (2) to the experimental points. The $n_e(I_{L_2},T)$ values that are obtained by this fitting procedure are shown in Fig. 6 for $T=5$, 8, and 12 K. It should be noted that the contribution of resonant excitation (I_{L_1}) to n_e is subtracted. This contribution for $I_{L_1}=3$ W/cm^2 is estimated to be $\sim10^9$ cm^{-2} by comparing the I_X/I_{X^-} obtained for $I_{L_2}<0.1$ mW/cm^2 and I_{L_1} with that obtained for I_{L_1} alone. Next we fit the $n_e(I_{L_2})$ data to a linear function and show these fittings by the solid lines in Fig. 6. For the three temperatures studied, we find that the fit is good except for the high photoexcitation intensities. This finding justifies the applicability of the noninteracting 2DEG model to determine the dependence of n_e on I_{L_2}.

We now consider the (X^-,e) scattering as the source of the linewidth increase and analyze its dependence on the 2DEG density and on temperature. We first calculate the Coulomb interaction matrix element between a pair of a free electron and a trion. Then, the scattering rate is calculated. We assume that the trion is free to move in the QW plane with an in-plane wave vector **K**. Although one might expect the trions to be able to recombine from any **K** state (imparting the extra momentum to the additional electron), examining the form factor connecting the bound and free-electron states in the recombination process reveals a dependence of $1/K^6$ that restricts this recombination process to small-K values only. We thus assume that in order to recombine radiatively the trion must scatter to the $K=0$ state. Figure 7 is a schematic description of the e, hh, and X^- dispersion curves and the wave-vector changes involved in the (X^-,e) scattering process. The (X^-,e) Coulomb interaction Hamiltonian is

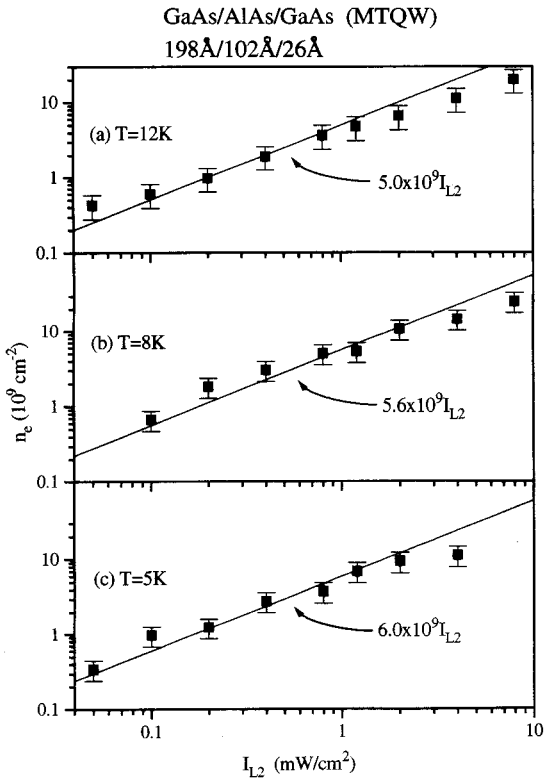

FIG. 6. $n_e(I_{L_2})$ values extracted from I_X/I_{X^-} by using the two-level model [Eqs. (1) and (2)]. The contribution of resonant excitation (I_{L_1}) to n_e is subtracted. The solid lines are approximated linear functions.

$$H=\frac{-e^2}{\epsilon|\mathbf{R}+\mathbf{r}-\mathbf{r}_e|}. \tag{3}$$

Here $\mathbf{R}$ is the X^- center-of-mass vector (in the QW plane), $\mathbf{r}$ is the additional bound electron position vector (with respect to $\mathbf{R}$), and $\mathbf{r}_e$ is that of the free electron. (ϵ is the dielectric constant.) The antisymmetrized wave function of the X^- in its $|1s,\mathbf{K}\rangle$ state and the electron in its $|\mathbf{k}\rangle$ state is

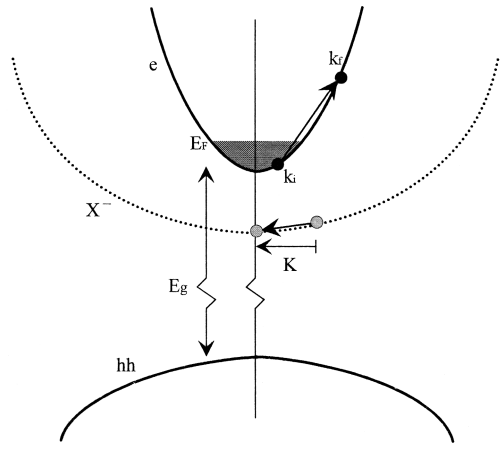

FIG. 7. Schematic description of the e, hh, and X^- dispersion curves and the wave-vector changes in the (X^--e) scattering process.

$$|(1s,\mathbf{K}),\mathbf{k}\rangle=\frac{1}{\sqrt{2}A}\{\exp[i(\mathbf{K}\cdot\mathbf{R}_1+\mathbf{k}\cdot\mathbf{r}_{e2})]\phi_{1s}(r_1) - \exp[i(\mathbf{K}\cdot\mathbf{R}_2+\mathbf{k}\cdot\mathbf{r}_{e1})]\phi_{1s}(r_2)\}. \tag{4}$$

We use the notation $\mathbf{R}_1,\mathbf{r}_1$ for the case of electron 1 being bound while $\mathbf{r}_{e2}$ is free (and vice versa). A is the normalization area. The X^- is approximated by a donorlike particle[12] with the additional bound electron in a $1s$ state having a Bohr radius of $a_{X^-}\sim 100$ Å. This donorlike X^- wave function is

$$\phi_{1s}(r)=\left(\frac{8}{\pi a_{X^-}^2}\right)^{1/2}\exp\left(-\frac{2r}{a_{X^-}}\right). \tag{5}$$

We consider scattering from an initial state $|(1s,\mathbf{K}),\mathbf{k}_i\rangle$ to a final state $|(1s,0),\mathbf{k}_f\rangle$ from which the trion recombines radiatively. Using the expansion

$$\frac{1}{|\mathbf{r}-\mathbf{r}_e|}=\frac{2\pi}{A}\sum_{\mathbf{q}}\frac{1}{q}\exp[i\mathbf{q}\cdot(\mathbf{r}-\mathbf{r}_e)], \tag{6}$$

we calculate the direct Coulomb interaction matrix element

$$U(K)=\langle(1s,K=0),\mathbf{k}_f|H|(1s,\mathbf{K}),\mathbf{k}_i\rangle = \frac{2\pi e^2}{\epsilon A(K+q_s)\left[1+\left(\frac{m_X}{4M}Ka_{X^-}\right)^2\right]^{3/2}}. \tag{7}$$

M and m_X are the X^- and X masses, respectively, and q_s is the screening wave vector. The (X^-,e) scattering rate is then given by

$$W=\frac{2\pi}{\hbar}\int\frac{d\mathbf{K}\,d\mathbf{k}_i}{\left(\frac{(2\pi)^2}{A}\right)^2}U(K)^2 f_{X^-}(K)f_e(k_i) \times[1-f_e(|\mathbf{k}_i+\mathbf{K}|)][1-f_{X^-}(K=0)] \times\delta\left[\frac{\hbar^2K^2}{2}\left(\frac{1}{M}-\frac{1}{m_e}\right)-\frac{\hbar^2}{m_e}\mathbf{k}_i\cdot\mathbf{K}\right]. \tag{8}$$

The f's are Fermi-Dirac distribution functions using the chemical potential given in Eq. (1). In order to fit Eq. (8) to the experimental results we treat $q_s(n_e)$ as a fitting parameter. The calculated $\Delta\Gamma=\hbar W$ values (for each experimental point) are interpolated by the smooth functions that are shown by the solid lines in Figs. 5(a), 5(c), and 5(e). This model is applicable to an interaction between charged, free particles. It is not expected to hold for electron-exciton scattering since the electron interaction with a neutral particle is short range (contact type). Indeed, as the experimental $\Delta\Gamma(n_e)$ values show, there is hardly any increment in the homogeneous exciton linewidth with increasing n_e [Figs. 5(b), 5(d), and 5(f)], in clear contrast to those of the trion. For the trion, the lowest 2DEG density value at which $\Delta\Gamma(n_{e,\min})$ shows a measurable increment is observed to decrease with increasing temperature: $n_{e,\min}\sim 2\times10^9$ cm^{-2} at $T=5$ K [Fig. 5(e)] and it decreases to $\sim 1\times10^9$ cm^{-2} at $T=8$ K [Fig. 5(c)]. At $T=12$ K [Fig. 5(a)] $\Delta\Gamma>0$ for the lowest n_e. A plausible explanation might be the existence of shallow localized electron states[13] that decrease the probability

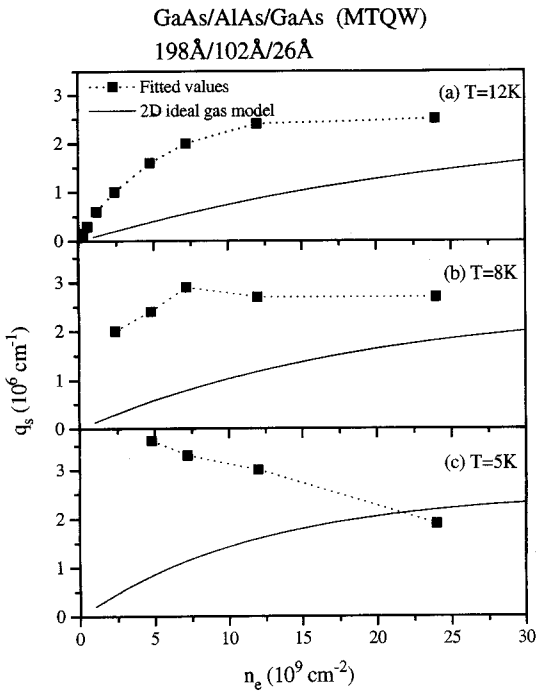

FIG. 8. Squares are values of $q_s(n_e)$ obtained by fitting the experimental X^- linewidth data of Figs. 5(a), 5(c), and 5(e) using the model given by Eqs. (7), (8). Solid lines are obtained by using the 2D ideal gas model [Eq. (9)].

of $(X^-$-$e)$ scattering. These localized states can be either thermally depopulated or saturated as n_e increases.

The $q_s(n_e)$ values obtained by fitting $\Delta\Gamma(n_e)$ using Eqs. (7) and (8) are given in Fig. 8 and are compared with those obtained by using the Thomas-Fermi approximation for an ideal two-dimensional gas:

$$q_s(n_e)=\frac{2\pi e^2}{\epsilon}\frac{dn_e}{d\mu}=\frac{2}{a_B}[1-e^{-E_f/k_BT}]. \qquad (9)$$

These functions are shown in Fig. 8 (solid lines) for the temperatures at which the experiments were done. While both are of the same order of magnitude, the q_s values extracted from fitting $\Delta\Gamma(n_e)$ are found to be larger than those calculated by using Eq. (9). We note that there is a distinct change in the $q_s(n_e)$ dependence when T increases [cf. Figs. 8(b) and 8(c)]. This indicates that the 2DEG screening has a complex dependence on both density (in the low-n_e range) and temperature. Moreover, the fitted q_s values asymptotically approach $\sim 2.5\times 10^6$ cm^{-1} for high-n_e values. Equation (9) predicts $q_s \rightarrow 2/a_B$ for $E_f \gg k_BT$ (i.e., in the $n_e \sim 10^{11}$ cm^{-2} range). Comparing this limit with the asymptotic value yields $a_B \sim 80$ Å. This value is slightly smaller than the exciton Bohr radius calculated using the effective masses.[14] Also, we note that the X^- binding energy (relative to the bare exciton) remains unchanged with increasing n_e. All these observations point at the complexity of the interacting electrons and the hole. It is plausible to assume that in the low-n_e range and at the temperatures of the experiments, the actual $q_s(n_e,T)$ values lie between the curves shown in Fig. 8. Further theoretical investigations are thus required.

IV. SUMMARY

We studied the spectral shape of $(e1$:hh$1)1S$ excitons (X) and that of the electron-bound excitons (trions, X^-) as a function of the 2DEG density in GaAs/AlAs QW's. The relative intensity of the X and X^- lines and their (homogeneous) linewidth are measured and used in order to determine the 2DEG density and the X^- dephasing by scattering with electrons. The experimental results are analyzed in terms of a model that assumes a mixed phase of free electrons, excitons, and trions. This phase is at an equilibrium state with a chemical potential that is dependent mainly on the 2DEG density. The trion, being a charged particle, scatters efficiently by the free electrons. We calculate the elastic scattering rate and relate it to the density-dependent X^- linewidth. This model treats the 2DEG screening wave vector as an adjustable parameter. Its dependence on n_e, for various temperatures, is extracted from the model fitting. Therefore, we demonstrate that the screening wave vector can be measured by spectroscopic means for low n_e and finite T.

ACKNOWLEDGMENTS

The work at Technion was done in the Barbara and Norman Seiden Center for Advanced Optoelectronics and was supported by the U.S.–Israel Binational Science Foundation, Jerusalem, Israel.

[1] S. Schmidt-Rink, D. S. Chemla, and D. A. B. Miller, Adv. Phys. **38**, 89 (1989).
[2] D. Heiman, Semicond. Semimet. **36**, 2 (1992).
[3] G. D. Sanders and Y.-C. Chang, Phys. Rev. B **35**, 1300 (1987).
[4] D. Huang, J. Chui, and H. Morkoc, Phys. Rev. B **42**, 5147 (1990).
[5] K. Kheng, R. T. Cox, Y. Merle d'Aubigne, F. Bassani, K. Saminadayar, and S. Tatarenko, Phys. Rev. Lett. **71**, 1752 (1993).
[6] G. Finkelstein, H. Shtrikman, and I. Bar-Joseph, Phys. Rev. Lett. **74**, 976 (1995).
[7] A. J. Shields, M. Pepper, D. A. Ritchie, M. Y. Simmons, and G. A. C. Jones, Phys. Rev. B **51**, 18 049 (1995).
[8] Arza Ron, H. W. Yoon, M. D. Sturge A. Manassen, E. Cohen, and L. N. Pfeiffer, Solid State Commun. **97**, 741 (1996).
[9] I. Galbraith, P. Dawson, and C. T. Foxon, Phys. Rev. B **45**, 13 499 (1992).
[10] J. Feldmann, M. Preis, E. O. Göbel, P. Dawson, C. T. Foxon, and I. Galbraith, Solid State Commun. **83**, 245 (1992).
[11] A. Manassen, E. Cohen, Arza Ron, E. Linder and L. N. Pfeiffer, Superlatt. Microstruct. **15**, 175 (1994).
[12] N. P. Sandler and C. R. Proetto, Phys. Rev. B **46**, 7707 (1992).
[13] I. Brener, M. Olszakier, E. Cohen, E. Ehrenfreund, Arza Ron, and L. Pfeiffer, Phys. Rev. B. **46**, 7927 (1992).
[14] M. Grundmann and D. Bimberg, Phys. Rev. B **38**, 13 486 (1988).